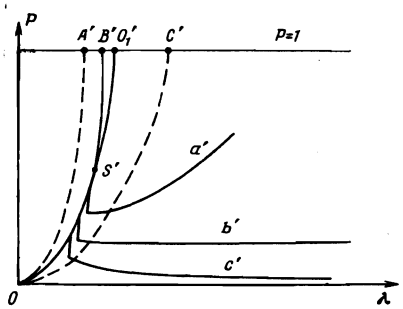

FIG. 7. The graphs of $P=P(\lambda)$ corresponding to the curves of Fig. 6.

core. Figures 6 and 7 show the solutions for the velocity and pressure with strong and weak discontinuities that have a uniformly expanding core (a piece of the Friedmann universe). In the same figures we show the inhomogeneous cosmological solutions (2.6) and (2.10) for the values of 0.125 and 0.75, respectively, of the parameter P_1.

[1]R. H. Dicke, P. J. E. Peebles, P. G. Roll, and D. T. Wilkinson, Astrophys. J. **142**, 414 (1965).
[2]L. D. Landau and E. M. Lifshitz, Teoriya Polya Nauka, 1972 (The Classical Theory of Fields, Pergamon Press, Oxford 1976).
[3]V. A. Skripkin, Zh. Prikl. Mekh. Tekh. Fiz. No. 4, 3 (1960); Astron. Zh. **38**, 192 (1961) [Sov. Astron. **5**, 143 (1961)].
[4]K. P. Stanyukovich, O. Sharshekeev, and V. Ts. Gurovich, Dokl. Akad. Nauk SSSR **165**, 510 (1965) [Sov. Phys. Dokl. **10**, 1030 (1966)].
[5]V. Ts. Gurovich, Dokl. Akad. Nauk SSSR **169**, 62 (1966) [Sov. Phys. Dokl. **11**, 569 (1967)].
[6]E. M. Lifshitz, Zh. Eksp. Teor. Fiz. **16**, 587 (1946).
[7]T. V. Ruzmaĭkina and A. A. Ruzmaĭkin, Zh. Eksp. Teor. Fiz. **59**, 1576 (1970) [Sov. Phys. JETP **32**, 862 (1971)].
[8]M. E. Cahill and A. H. Taub, Comm. Math. Phys. **21**, 1 (1971).
[9]N. R. Sibgatullin, Dokl. Akad. Nauk SSSR **187**, 531 (1969) [Sov. Phys. Dokl. **14**, 619 (1970)].
[10]V. A. Skripkin, Dokl. Akad. Nauk SSSR **136**, 791 (1961) [Sov. Phys. Dokl. **6**, 115 (1961)].
[11]K. P. Stanyukovich, Zh. Eksp. Teor. Fiz. **43**, 199 (1962) [Sov. Phys. JETP **16**, 142 (1963)].
[12]I. M. Khalatnikov, Zh. Eksp. Teor. Fiz. 27, 529 (1954).
[13]N. R. Sibgatullin, Kandidatskaya Dissertatsiya (Candidate's Dissertation), MGU (1969).
[14]L. P. Sedov, Metody Podobiya i Razmernosti v Mekhanike (Similarity and Dimensional Methods in Mechanics), Nauka (1967).
[15]L. I. Sedov, Prikl. Mat. Mech. **36**, 3 (1972).
[16]B. J. Carr and S. W. Hawking, Mon. Not. R. Astron. Soc. **168**, 399 (1974).

Translated by Julian B. Barbour

Particle-like solutions of the scalar Higgs equation

T. I. Belova, N. A. Voronov, I. Yu. Kobzarev, and N. B. Konyukhova

Institute of Theoretical and Experimental Physics

(Submitted 18 November 1976; resubmitted 11 July 1977)
Zh. Eksp. Teor. Fiz. **73**, 1611–1622 (November 1977)

The properties of particle-like solutions of the scalar Higgs equation are considered. These solutions should correspond in the Vinciarelli-Drell model to gluon-type mesons that contain no quark-antiquark pair.

PACS numbers: 11.10.Qr

I. INTRODUCTION

According to present indications, the effective mass of the quarks inside hadrons is small; in particular, for non-strange quarks it turns out to be of the order of 5–10 MeV.[1] On the other hand, free quarks either do not exist at all or their concentration in matter and their production cross section are small.[2]

This situation makes it necessary to resort to models in which the quarks interact with fields of the boson type, and this interaction is such that a small region $\sim 10^{-13}$ cm is produced, in which the quarks move with velocity $\sim c$ and with a mass on the order of zero, whereas in the remaining space they can either not be present at all, or have their very large effective mass. Models of the first type[3] correspond to absolute confinement, while in the model of the second type the free quarks should be observable. If the data of LaRue, Fairbank, and Hebbard[4] were to be confirmed, then we should give preference to the models of the second type. The simplest of these models is the Vinciarelli-Drell model,[5] in which the quark field q interacts with the scalar Hicks field u described by the equation[1)]

$$\Box u=4\lambda^2 u(\eta^2-u^2). \tag{1.1}$$

For (1.1), vacuum corresponds to $u=\pm\eta$. If the interaction of the quark with this field takes the form $fu\bar{q}q$, then the quark outside the hadron has a mass $f\eta$, and if $f\eta \gg 1$ GeV, then the free quark has a small effective mass.

Since arguments exist favoring the assumption that the interaction of the quarks is due to colored Yang-Mills

0038-5646/77/4605-0846$02.40

fields,[1] introduction of another scalar field seems unjustified. One might assume, however, that the appearance of the two types of regions is connected with a phase transition for the Yang-Mills fields,[6] and then the field u could describe a condensate.

Introduction of boson fields that cause interaction of quarks (gluon fields) means that in addition to the mesons of the ordinary type, which correspond to the $q\bar{q}$ pairs, there should exist also gluon states (gluonium) described by the quantum particle-like solution of the equations of the gluon field. Within the framework of the confinement hypothesis, the gluonium should be a bound state of two or more Yang-Mills gluons, since colored states are forbidden, and to construct a white state we need two or more gluons. In the Vinciarelli-Drell model[5] there exist quanta of the field u with mass ηf, but in addition, by virtue of the nonlinearity of (1.1), particle-like solutions are also possible, corresponding to a bound state of many such quanta. In this article we shall consider classical particle-like solutions of (1.1), which correspond to states of this type. Equation (1.1) and its solutions were considered earlier in[7-12].

It appears that Eq. (1.1) cannot be completely integrated already in one dimension, since the number of integrals of motion for (1.1) is finite.[13] Therefore, in contrast to the sine-Gordon equation, while the spectrum and the solution of the Cauchy problem can be completely described,[14] there is no systematic method of analysis here. This pertains all the more to three dimensions. In this paper we propose a number of analytic models that describe particular particle-like solutions of (1.1) and their properties. The models were verified in numerical experiments whose results are reported below.

We call a solution particle-like if the energy density ε, given by

$$\varepsilon=\tfrac{1}{2}(\partial u/\partial t)^2+\tfrac{1}{2}(\nabla u)^2+(u^2-1)^2, \tag{1.2}$$

is localized for this solution in a finite region in the sense that ε tends to zero at infinity and that the total energy E, equal to

$$E=\int \varepsilon\, dV, \tag{1.3}$$

is finite. Formulas (1.1)–(1.3) can be used for spaces with arbitrary numbers of dimensions, provided that ∇ and dV are suitably defined.

It is known[15] that Eq. (1.1), in the case of $n>1$ spatial dimensions, have no stable static solutions. We consider here the properties of quasi-periodic particle-like solutions of (1.1), i.e., localized pulsating formations with lifetimes $\tau \gg T$, where T is the period of the oscillations. The amplitude of these pulsations can decrease as a result of radiation. At the present time, pulsating states of this type have been observed in both one-dimensional and three-dimensional spaces.

For Eq. (1.1) in the case of three dimensions, there are two known types of quasi-periodic solutions: solutions of the type of pulsating bubbles,[16] and solutions of the type of isochronous excitations which were considered in[17,18]. We discuss below the properties of these solutions, the connection between them, and the question of their lifetime.

In the numerical experiments we investigated the solutions of (1.1) for the three-dimensional and one-dimensional cases at different sets of u and u_1 at the initial instant of time. The formulation of the Cauchy problem for each case is given in the corresponding sections. The numerical solution of the Cauchy problem, in contrast to[16], was obtained by the method of characteristics.[19] This method of calculation has the following advantages over the program used earlier.

a) A high accuracy of calculation, and in particular, the energy integral is well conserved even if a rather loose grid is chosen. This energy integral oscillates slowly about its initial value in all the calculations cited in the present paper, and the amplitude of these oscillations does not exceed 0.1% of the initial value of the energy.

b) The solution automatically assumes a value +1 in the limit of large r, and this makes it possible to calculate correctly the energy flux at infinity.

2. COMPRESSION OF A SPHERICAL BUBBLE

The properties of the planar solutions of Eq. (1.1) were considered in detail in[10], where they were called walls. These walls could move with velocity v perpendicular to their surface. A wall parallel to the (x, y) and moving with velocity v corresponds to the solution

$$u=\mathrm{th}\,[\gamma\overline{2}(z-vt)/(1-v^2)^{1/2}]. \tag{2.1}$$

The wall has a surface energy density concentrated in a layer of thickness $l\sim(1-v^2)^{1/2}$ and equal to

$$\mu'=\mu/(1-v^2)^{1/2}, \tag{2.2}$$

while μ is the energy density of the resting wall, equal to $4\sqrt{2}/3$ in the system of units employed here.

We consider now a system, called in[10] a bubble, it is made up of a spherical wall. Inside the bubble $u=-1$, and outside $u=+1$. If the sphere radius $R\gg 1$, then Eq. (2.2) is valid for the surface energy density. From energy considerations it is obvious that the bubble will contract.

The action for Eq. (1.1) is given by

$$S=\int \mathcal{L}(u)\, d^4x, \tag{2.3}$$

where

$$\mathcal{L}(u)=\tfrac{1}{2}(\partial u)^2-(u^2-1)^2.$$

At $R\gg 1$ we can integrate in (2.3) over the shell of the bubble, thus obtaining the action[20]

$$S=-4\pi\mu\int R^2(1-\dot{R}^2)^{1/2}\, dt, \tag{2.4}$$

corresponding to the effective Lagrangian

$$\mathcal{L}(R)=-4\pi\mu R^2(1-\dot{R}^2)^{1/2}. \tag{2.5}$$

From (2.4) follows the equation of motion

$$d^2R/dt^2=-2(1-\dot{R}^2)/R \qquad (2.6)$$

with an energy integral

$$E=4\pi\mu R^2/(1-\dot{R}^2)^{1/2}. \qquad (2.7)$$

The solution of (2.6) with the initial condition $R(0)=R_0$ is of the form

$$R=R_0\,\mathrm{cn}(\sqrt{2}t/R_0,\ 1/2), \qquad (2.8)$$

where $cn(x, \frac{1}{2})$ is the elliptic cosine with modulus $k^2=\frac{1}{2}$.

We have investigated with a computer the compression of the bubble, starting directly from the wave equation (1.1). The initial conditions specified at the instant $t=0$ were

$$u(r,\ 0)=\mathrm{th}\,\sqrt{2}(r-R_0),\quad u_t(r,\ 0)=0. \qquad (2.9)$$

If the radius R of the bubble is defined as the distance from the center to the sphere on which u vanishes, then the dependence of R on t for the initial conditions (2.9) (Fig. 1) is well described by (2.8) up to $R(t)\sim 1$, even though the solution u itself is already strongly deformed at the corresponding t and differs noticeably from that of a contracting hypertangent.

3. REFLECTION

In[16] it was shown by a numerical experiment that after the collapsing bubble reaches $R\sim l$, reflection takes place and the contraction gives way to expansion. Whereas the contraction process is well described by the inverted equation (2.6), to describe the reflection it is necessary to turn directly to Eq. (1.1).

It is easiest to explain the reflection mechanism in the one-dimensional case. The ensuing simplification is connected with the fact that it is possible here to take two walls that move towards each other with arbitrary velocities, and in planar geometry these velocities hardly increase with time so long as the distance between the walls is large in comparison with l. We present below the results of numerical calculations in which we verified the simple hypothesis concerning the reflection mechanism.

So long as the two walls are separated by a large distance, the solution can be represented in the form

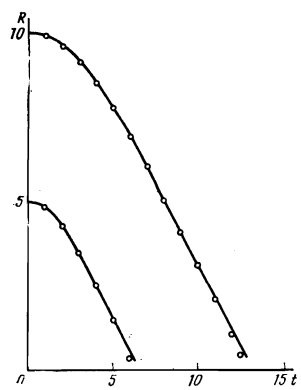

FIG. 1. Compression of bubble. Solid line—the function $R(t)$ calculated from formula (2.8), points—results of numerical experiment.

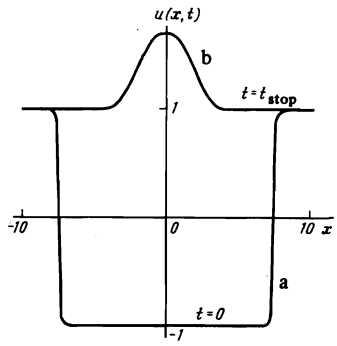

FIG. 2. Reflection in one-dimensional case: a) initial condition $u(x, 0)$, b) $u(x, t_{stop})$ at the instant of stopping.

$$u(x,t)=\mathrm{th}\left[\sqrt{2}\frac{x+vt-x_0}{(1-v^2)^{1/2}}\right]+\mathrm{th}\left[\sqrt{2}\frac{-x+vt-x_0}{(1-v^2)^{1/2}}\right]+1, \qquad (3.1)$$

where

$$v>0,\quad x_0>0,\quad x_0-vt\gg 1.$$

The results of the numerical experiments can be interpreted by starting from the hypothesis that the walls retain their individuality also when the distance between them is of the order of the wall width and even when the terms overlap. If the solution u prior to the overlap was of the form shown in Fig. 2a, it takes after the overlap the form of Fig. 2b. Since the central part has energy, the walls will ultimately stop. At the instant of stopping, the solution takes the form

$$u=\mathrm{th}[\sqrt{2}(x+L_{stop})]+\mathrm{th}[\sqrt{2}(-x+L_{stop})]+1,\ L_{stop}>0. \qquad (3.2)$$

At this instant of time the solution has an energy[2)]

$$V(L_{stop})=\int[1/2(u_x)^2+(u^2-1)^2]dx, \qquad (3.3)$$

where u must be replaced by (3.2). Then L_{stop} is determined from the condition

$$V(L_{stop})=E_0, \qquad (3.4)$$

where E_0 is the initial energy, equal to $2\mu/(1-v^2)^{1/2}$.

We have obtained $u(x, t_{stop})$ independently by solving (1.1) numerically with the initial condition (3.1). From the collision model described above and from the numerical calculations it follows that the instant of stopping corresponds to the maximum of $u(0, t)$.

In Fig. 3 are compared the $u(x, t_{stop})$ curves obtained

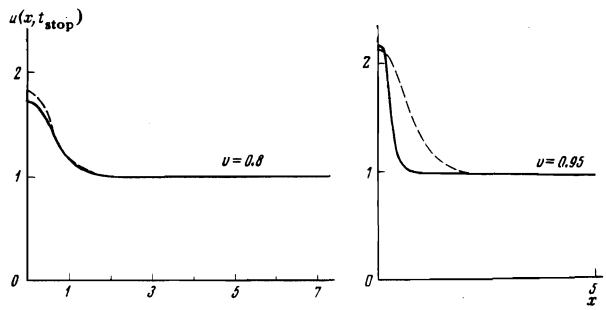

FIG. 3. Comparison of the reflection model with a numerical experiment. Solid line—the function u at the instant of stopping, dashed—the function u obtained in the reflection model.

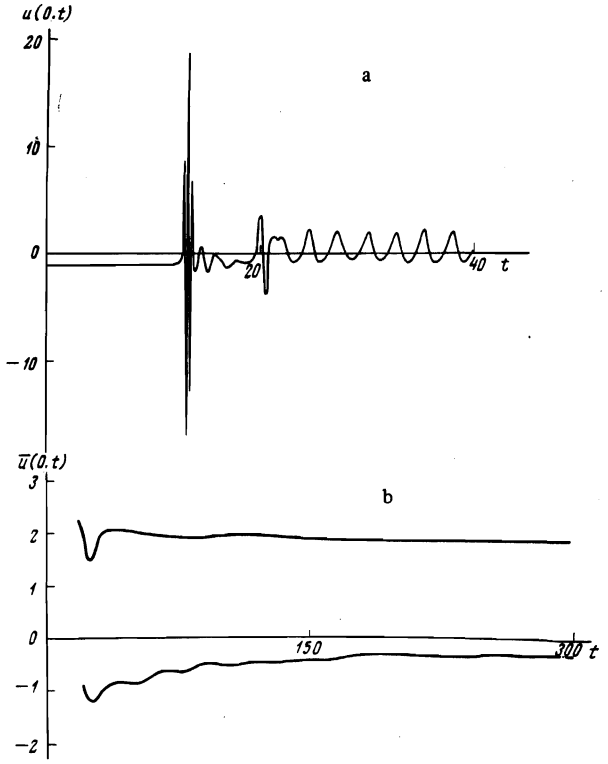

FIG. 4. Evolution of a bubble with $R_0 = 10$; a) dependence of u on the time at the point $r = 0$, b) envelopes of the maxima and minima of the produced isochrone.

in the collision model described above with those determined numerically. It is seen that our model describes very well the collision at not too large velocities; at $v > 0.8$, the collision mechanism changes.

In the three-dimensional case the situation is much more complicated. The reason is that by the instant of the impact the walls are strongly deformed[16] and a rather appreciable oscillations which attenuate exponentially at infinity, appear against the background of the contracting hypertangent. One can assume that qualitatively the overlap hypothesis describes the reflection in this case, too. Then the overlap of the oscillations in the function $u(r, t)$ when the bubble walls collide might explain the $u(0, t)$ oscillations observed in the numerical experiment (Fig. 4a).

4. RADIATION AND LIFETIME

The accuracy of the program of[16] was insufficient to shed light on the question of the bubble lifetime. Recently a group at JINR[17] was able to solve this problem. It turned out after reflection and the subsequent expansion, the bubble stops without reaching its initial radius R_0 and emits at that instant an appreciable fraction of its energy in the form of spherical waves. Our calculations, performed by the new procedure, agree with the results of[17].

It is interesting that at $R_0 = 5$, after the first oscillation the bubble stops at $R_1 = 3.8$ and then, during the next succeeding oscillations, it returns to approximately the same position. A similar picture was observed also in[17] for $R_0 = 4$. We have verified the interval of the values $3 \leq R_0 \leq 5$ and show in Fig. 5 the ratio R_1/R_0 as a function of R_0, where R_1 is the radius of the bubble after the first stopping. We see that there exists a certain interval of the values of R_0, at which the bubble returns with sufficient accuracy to the initial position. We shall discuss the interpretation of this phenomenon in Sec. 7.

5. ISOCHRONES

As first established by a numerical experiment,[17] after the oscillating bubble is rid of its energy, there remains a particle-like system that oscillates about the level $u = 1$ (-1). These oscillations turn out to be very long-lived. In[17] they observed about 10^3 pulsations, and an analogous picture was observed also by us.

A similar state was obtained also in the one-dimensional case.[21] The lifetimes of these states should also be finite because of radiation. This radiation was observed in[22], and a value $\sim 10^3\ T$ obtained for the lifetime, where T is the period of the oscillations.

A characteristic property of these formations is that at small amplitudes the period is independent, accurate to $O(\varepsilon^2)$, of the amplitude (it is constant), we therefore propose to call pulsating states of this type "isochrones."[18]

The periodic solutions for the one-dimensional case were sought[12] in the form of series in the parameter ε, which determines the amplitude of the oscillations ($\varepsilon - 0$ corresponds to an amplitude that tends to zero). It was noticed in[18] that these solutions can describe the isochrone states that are observed in the numerical experiment. An analogous solution was also obtained there for three-dimensional space.

It appears that these series are asymptotic in ε. This is indicated both by the growth of the coefficients of the series with a power of ε by the fact that the energy radiation is not described by such a series. The latter would be natural if the radiation flux were proportional to $e^{-c/\varepsilon}$, where c is the numerical constant.

To obtain the indicated series, it is convenient to changeover in (1.1) to the new variables

$$u = 1 + w, \quad \tau = \frac{2\sqrt{2}\,t}{(1+\varepsilon^2)^{1/2}}, \quad \rho = \frac{2\sqrt{2}\,er}{(1+\varepsilon^2)^{1/2}}. \tag{5.1}$$

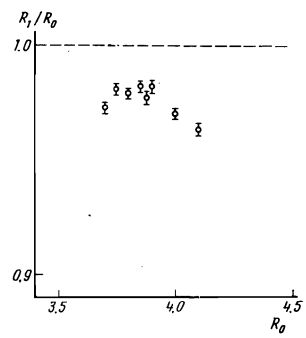

FIG. 5. Dependence of the ratio R_1/R_0 on the initial radius R_0.

We will represent the function W in the form of a series in the parameter ε:

$$w=\varepsilon^2 g_0(\rho)+\sum_{n=1}^{\infty}[\varepsilon^{2n-1}f_{2n-1}(\rho)\sin(2n-1)\tau+\varepsilon^{2n}g_{2n}(\rho)\cos 2n\tau], \qquad (5.2)$$

and the functions f_i and u_i are also expanded in powers of ε^2

$$f_i(\rho)=\sum_{j=0}^{\infty}f_i^{(j)}(\rho)\varepsilon^{2j}, \quad g_i(\rho)=\sum_{j=0}^{\infty}g_i^{(j)}(\rho)\varepsilon^{2j}. \qquad (5.3)$$

It can be shown that all the functions $f_i^{(j)}(\rho)$ and $g_i^{(j)}(\rho)$ can be expressed in terms of $f_1^{(0)}$, which in turn satisfies the equation

$$\Delta_\rho f_1^{(0)}-f_1^{(0)}+{}^3/_2[f_1^{(0)}]^3=0 \qquad (5.4)$$

with boundary conditions

$$f_1^{(0)}(0)<\infty, \quad f_1^{(0)}(\infty)=0, \quad \left.\frac{df_1^{(0)}}{d\rho}\right|_{\rho=0}=0.$$

It has been shown[23] that Eq. (5.4) has solutions with n nodes (zeroes) $n=0,1,\ldots$, satisfying the boundary conditions.

Confining ourselves to the expansion term linear in ε, we have

$$w=\varepsilon f_1^{(0)}\left(\frac{2\sqrt{2}\,\varepsilon r}{(1+\varepsilon^2)^{1/4}}\right)\sin\frac{2\sqrt{2}\,t}{(1+\varepsilon^2)^{1/4}}. \qquad (5.5)$$

According to (5.5), the period of the oscillations of the isochrone is

$$T=\frac{\pi}{\sqrt{2}}(1+\varepsilon^2)^{1/4}. \qquad (5.6)$$

The same constant ε determines also the amplitude A of the oscillations at zero:

$$A=\varepsilon f_1^{(0)}(0). \qquad (5.7)$$

For the ground state of Eq. (4), which has no zeroes, we have $f_1^{(0)}(0)\approx 3.6$. We compare now formulas (5.6) and (5.7) with the numerical calculations. For example, the state produced upon collapse of a bubble with initial radius $R_0=10$ (see Fig. 4a). The period of the oscillations of this isochrone is $T=2.5$; this yields a value 0.5 for ε, and then $A=1.8$. The experimental amplitude is $A_{exp}\approx 1.5$. The agreement with (5.7) can be regarded as satisfactory, since the series (5.2) is asymptotic and ε is comparable with unity.

We note that in the course of its evolution this isochrone does not experience the amplitude pulsations (see Fig. 4b) that were observed in[24]. The amplitude pulsations are therefore not a characteristic property of isochrones and appear only in the case of a definite choice of the initial conditions.

For the isochrone that is produced when a bubble with $R_0=5$ is collapsed, the picture is more complicated (Fig. 6). If we start with the period, then the value of ε calculated from (5.6) is 0.2. But the amplitude of the isochrone produced immediately after the last pulsation is too large to be described by expression (5.7). The behavior of the isochrone can be understood by assuming that the collapse of the bubble is followed by formation of an isochrone with $f_1^{(0)}$ having a single zero (in contrast to the case with $R_0=0$, when the isochrone is produced directly in the ground state), and this formation is disintegrated quite rapidly, going over into the ground state of the isochrone without a change of the period. An analysis of the spatial distribution of the function $u(r, t_{max})$ at the instant when the maximum amplitude is reached before and after the transition agrees with such a picture. We note that when the spatial distribution of the function $u(r, t_2)$ (see Fig. 6b) after the transition was compared with the series (5.2), we used terms $\sim\varepsilon^2$, thereby improving the agreement with the experimental curve. This operation is valid, inasmuch as the term $\sim\varepsilon^2$ is much smaller than the term $\sim\varepsilon$. It is incorrect to take into account for the isochrone after the transition terms that are quadratic in ε, since the terms $\sim\varepsilon^2$ for $f_1^{(0)}$ with a single node are comparable with the linear term.

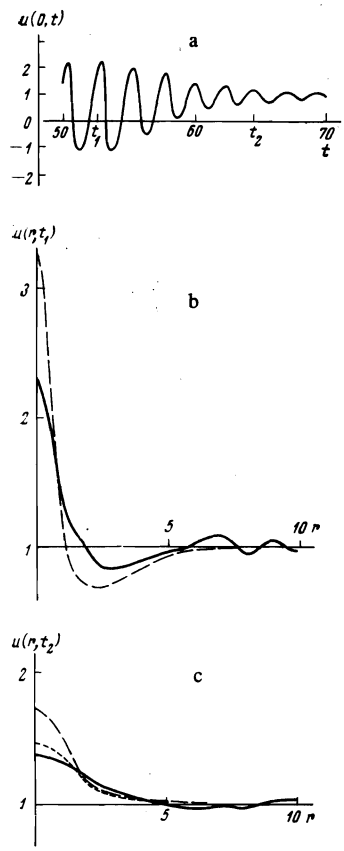

FIG. 6. Behavior of the isochrone produced following the collapse of a bubble with $R_0=5$. a) The function u at the point $r=0$; b), c) spatial distribution of the isochrone before and after the transition, respectively. Solid line—result of numerical experiment; dashed—linear fit; short dashes—approximation quadratic in ε.

6. PRODUCTION OF QUASIPARTICLES

In the case of integrable systems, there is a known method[25] of separating the contribution of the particle-like state (solitons) for any initial condition. Since no such methods have been obtained for a non-integrable equation, it is expedient to investigate numerically the dependence of the production of the quasiparticle states on the initial conditions. It was shown earlier that if a state of the bubble type is specified at the initial instant

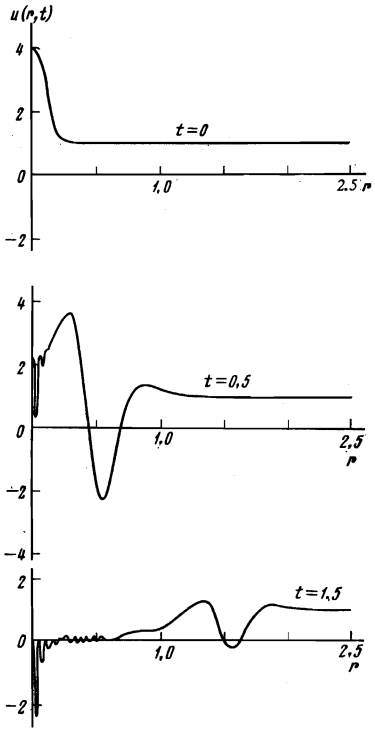

FIG. 7. Evolution of the field with initial condition (6.2) at $\gamma = 0.35$.

of time, this leads to formation of long-lived isochrones. Obviously, the result does not depend on which of the stages of the pulsations is chosen to be the initial condition.

We have considered, besides the bubble, initial conditions of the type

$$u(r, 0) = \gamma^{-1} e^{-\alpha r^2} + 1, \quad u_t(r, 0) = 0, \tag{6.1}$$

where $\alpha > 0$, and γ can be either positive or negative. Figure 7 shows the result of the numerical calculations with the initial conditions (6.1). It is seen that no isochrone with large amplitude is produced.

Analogous calculations were performed also for the one-dimensional case. We specified the following initial values:

$$u(x, 0) = 1 + \gamma^{-1} e^{-\alpha x^2}, \quad u_t(x, 0) = 0. \tag{6.2}$$

Isochrone production was observed at $\gamma = 1.0$, 1.2, 2.0 and $\alpha = 10$.

We note that (6.2) approximates well the isochrone at the instant of the stopping. When $u(x, 0)$ was chosen to differ substantially from (6.2), no isochrone production was observed.

7. CONCLUSION

Let us examine some conclusions that follow from the results described above.

1. From the results of Secs. 2 and 3 it follows that the described motion of a wall that has been curved by an action of the type (2.5) is of limited applicability. It does not hold at curvature radii $R \sim l$, where l is the wall thickness, and does not describe at all the reflections tions of the walls. It is obvious that this conclusion does not depend on the spherical geometry used by us to simplify the calculations. We can then easily write down the convoluted action also for an arbitrary wall, in the form

$$S = -\nu \int (1 - v_\perp^2)^{1/2} (g_{11} g_{22} - g_{12}^2)^{1/2} \, du \, dv \, dt, \tag{7.1}$$

where u and v are arbitrary curvilinear coordinates on the wall surface, and $g_{ik}(u, v)$ is a metric tensor. Obviously, the conditions for the applicability of (7.1) are the same as in the spherical case.

The transition from the field action $S = \int \mathcal{L}(u) \, d^4x$ to the action (7.1) is analogous to the transition from the field action to the Nambu action

$$S = -\nu \int (1 - v_\perp^2)^{1/2} \frac{ds}{du} du \, dt, \tag{7.2}$$

used in the theory of strings.[3)] It is natural to conclude that the description (7.2) of string dynamics likewise has a limited region of applicability. It is likely that the difficulties that arise in the string theory based on (7.2) or on its generalizations are connected precisely with this circumstance.

2. The results of the numerical experiments described in Sec. 3 show that the collision of the walls is described by a simple model, according to which the colliding walls "preserve their individuality" even in the case of a noticeable overlap. The grounds for such a behavior in a non-integrable system are not clear to us; on the face of it, the walls should have been strongly deformed by the interaction. It is possible that the reason why the model is successful is that the form (3.2) for $u(f, t)$ has turned out to be a successful trial function that minimizes the action with good accuracy.

3. It can be regarded as established that metastable pulsating solutions of equations (1.1) exist and can be expanded in asymptotic series (at sufficiently low amplitudes). We regard it as likely that states with sufficiently large lifetimes exist also at larger amplitudes. An argument favoring this assumption is the nonmonotonic dependence of I_1/I_0 on R (see Sec. 4). A possible explanation of this phenomenon is that at these values of R_0 the initial condition specified by us turns out to be closest to $u(r, 0)$ corresponding to the metastable solution of the Higgs equation.

4. A comparison of the results of Secs. 4 and 6 indicates that the production of particle-like states for non-integral equations depends in non-trivial fashion on the initial conditions.

5. If the Vinciarelli-Drell model[5] is valid for the description of hadrons, then the particle-like solutions considered by us should correspond to scalar mesons of an unusual type (containing no quark-antiquark pairs

in first-order approximation). An experimental investigation of the question of the existence of such mesons can yield important information on the structure of hadrons. Of course, mesons of this type (gluon clusters) can be described also by other models, including the standard one (chromdynamics of colored quarks and of colored Yang-Mills fields), so that experimental observation of gluon clusters can by itself not yet be regarded as a confirmation of the Vinciarelli-Drell model.

One of us (N. B. K.) thanks V. M. Borisov for calling attention to the method of characteristics for the solution of Eq. (1.1).

[1)]Equation (1) reduces by a scale transformation to the form

$$u = 4u(1-u^2)\,, \qquad (1.1')$$

which will be used hereafter.

[2)]This function was first obtained in[21].

[1]M. Gell-Mann, Elementary particles, Preprint Princeton, 1974.
[2]L. G. Landsberg, Usp. Fiz. Nauk **109**, 695 (1973) [Sov. Phys. Usp. **16**, 251 (1973)].
[3]A. Chodos, R. L. Jaffe, K. Jonson, C. B. Thorn, and V. F. Weiskopf, Phys. Rev. D 9, 3471 (1974).
[4]G. S. La Rue, W. M. Fairbank, and A. F. Hebard, Phys. Rev. Lett. 38, 1011 (1977).
[5]P. Vinciarelli, Nucl. Phys. B 89, 463 (1975); W. A. Bardeen, M. Chanowitz, S. D. Drell, M. Weinstein, and T.-M. Yan, Phys. Rev. **D11**, 1094 (1975).
[6]C. G. Callan, R. F. Dashen, and D. J. Gross, Phys. Lett. B **66**, 375 (1977).
[7]R. Finkelstein, R. Le Levier, and M. Ruderman, Phys. Rev. **83**, 326 (1951); J. Goldstone, Nuovo Cimento **19**, 154 (1961).
[8]P. W. Higgs, Phys. Rev. **154**, 1156 (1966).
[9]T. D. Lee and G. C. Wick, Phys. Rev. D 9, 2291 (1974).
[10]Ya. B. Zel'dovich, I. Yu. Kobzarev, and L. B. Okun', Zh. Eksp. Teor. Fiz. 67, 3 (1974) [Sov. Phys. JETP 40, 1 (1975)].
[11]A. M. Polyakov, Pis'ma Zh. Eksp. Teor. Fiz. 20, 430 (1974) [JETP Lett. 20, 194 (1974)].
[12]R. Dashen, B. Hasslacher, and A. Neveu, Phys. Rev. D **11**, 3424 (1975).
[13]P. P. Kulish, Teor. Mat. Fiz. **26**, 193 (1976).
[14]L. A. Lakhtadzhyan and L. D. Fadeev, Teor. Mat. Fiz. **21**, 160 (1974).
[15]G. H. Derrick, J. Math. Phys. 5, 1252 (1964).
[16]N. A. Voronov, I. Yu. Kobzarev, and N. V. Konyukhova, Pis'ma Zh. Eksp. Teor. Fiz. 22, 590 (1975) [JETP Lett. 22, 290 (1975)].
[17]I. L. Bogolyubskiĭ and V. G. Makhan'kov, Pis'ma Zh. Eksp. Teor. Fiz. 24, 15 (1976) [JETP Lett. 24, 12 (1976)].
[18]N. A. Voronov and I. Yu. Kobzarev, Pis'ma Zh. Eksp. Teor. Fiz. 24, 576 (1976) [JETP Lett. 24, 576 (1976)].
[19]I. S. Berezin and N. P. Zhidkov, Metody vychisleniĭ (Calculation Methods), 2, Fizmatgiz, 1960.
[20]M. B. Voloshin, I. Yu. Kobzarev, and L. B. Okun', Yad. Fiz. 20, 1229 (1974) [Sov. J. Nucl. Phys. 20, 644 (1975)].
[21]A. E. Kudrayavtsev, Pis'ma Zh. Eksp. Teor. Fiz. 22, 178 (1975) [JETP Lett. 22, 82 (1975)].
[22]B. S. Getmanov, Pis'ma Zh. Eksp. Teor. Fiz. 24, 323 (1976) [JETP Lett. 24, 291 (1976)].
[23]G. Ryder, Pacific J. Math. 22, 477 (1967).
[24]I. L. Bogolyubskiĭ and V. G. Makhan'kov, Pis'ma Zh. Eksp. Teor. Fiz. 25, 120 (1977) [JETP Lett. 25, 107 (1977)].
[25]V. E. Zakharov, in: I. A. Kunin, Teoriya uprugikh sred s mikrostrukturoĭ (Theory of Elastic Media with Microstructure), Nauka, 1975.
[26]I. Yu. Kobzarev, Materials of the Third ITEP School, No. 1, Atomizdat, 1975, p. 27.

Translated by J. G. Adashko